05,10

Solitons in the semi-bounded two-sublattice ferrimagnet

© V.V. Kiselev[1,2]

[1] M.N. Mikheev Institute of Metal Physics of the Ural Branch of the Russian Academy of Sciences, Yekaterinburg, Russia
[2] Ural Federal University named after the first President of Russia B.N. Yeltsin, Institute of Physics and Technology of Ural Federal University, Yekaterinburg, Russia

E-mail: kiseliev@imp.uran.ru

Received March 17, 2025
Revised March 23, 2025
Accepted March 24, 2025

The new soliton solutions of the model of semi-bounded ferrimagnet with two crystallographycally different magnetic sublattices are found and analyzed in the exchange approximation. The boundary conditions for free surface spins on the edge of the sample are taken into account. It is established, that the localization of solitons near the boundary of the sample is impossible at such conditions. During the collision of the moving solitons with the edge of the sample their cores undergo significant changes, which are accompanied by remagnetization of the medium near the sample surface. After the reflection of solitons from the surface, when moving inside the sample, the soliton cores acquire the stationary form, typical for the precessing solitons of the unbounded medium. The changes of the internal precession phases and shifts of the soliton centers after the reflection from the sample boundary are calculated.

Keywords: solitons, Landau–Lifshitz equation, ferrimagnets.

DOI: 10.61011/PSS.2025.04.61267.51-25

1. Introduction

The simplest model of a ferrimagnet contains two magnetic sublattices with magnetizations $\mathbf{M}_1(\mathbf{r}, t)$ and $\mathbf{M}_2(\mathbf{r}, t)$, where $\mathbf{r}$ and t are the radius vector and time, $\mathbf{M}_i^2 = M_{0i}^2 = \text{const}$ $(i = 1, 2)$, $M_{01} \neq M_{02}$. In the ground state, the vectors $\mathbf{M}_1$ and $\mathbf{M}_2$ are antiparallel. However, there is an uncompensated magnetization of the medium: $\mathbf{M} = \mathbf{M}_1 + \mathbf{M}_2 \neq 0$. The presence of two non-equivalent magnetic sublattices with strong geometric nonlinearity of fields $\mathbf{M}_{1,2}(\mathbf{r}, t)$ complicates the theoretical description of ferrimagnets. The Landau–Lifshitz equation of a single-lattice ferromagnet with magnetization $\mathbf{M}(\mathbf{r}, t)$ is often used to simplify the problem. This approximation is justified when the vectors $\mathbf{M}_1$ and $\mathbf{M}_2$ remain antiparallel in the excited states of the medium: $\mathbf{M}^2 = (M_{01} - M_{02})^2 = \text{const}$ or when the magnetizations of the sublattices differ markedly in magnitude [1,2]. Near the compensation point of sublattice magnetizations, ferrimagnets inherit the additional properties of antiferromagnets [3,4], due to the so-called „exchange enhancement“ of their dynamical properties. Then they gain a number of advantages over ferromagnets. First, having magnetic structure and high susceptibility to external fields, ferrimagnets have small magnetization and do not produce large magnetostatic fields. This makes them easier to describe from theoretical point of view. Ferrimagnetic particles interact weakly with each other from an applied point of view. Therefore, it is possible to create dense arrays of particles in which the long-range dipole-dipole interaction does not prevent the use of the bistable states of an individual particle to record information. Second, the characteristic frequencies of ferrimagnets, and hence the characteristic switching frequencies between different magnetic states, are several orders of magnitude higher than those of typical ferromagnetic materials (see for example [5,6]). This opens up the prospect of creating highspeed devices that no longer operate in the gigahertz (as ferromagnets do), but in the tetrahertz range. Possible applications of tetrahertz waves include applications in 4*G* and 5*G* — telecommunications systems and space communications, security and search for illicit materials, biology and medicine, information technology, and ultrafast data processing [7]. Finally, ferrimagnetic order in semiconductors is observed much more frequently and under much milder conditions than ferromagnetic ordering, making it possible to combine the advantages of both electronics (fast performance, easy controllability) and spintronics (high sensitivity, low power consumption) in the same device. In addition, ferrimagnets can have metallic conductivity, allowing the use of standard magnetoresistance effects to read signals in information systems or to convert the energy of spin oscillations into alternating electric current. Equally as important, modern methods of growing single crystals on substrates make it possible to vary the magnetic anisotropy and obtain ferrimagnetic materials with any pre-determined properties [6,8].

The mentioned features of ferrimagnetic materials are extremely useful for applications, the theoretical description of the nonlinear dynamics of ferrimagnets is an urgent task. Modern methods of soliton theory open new possibilities for

its solution. It is found that the Landau–Lifshitz equations for the magnetizations of a two-sublattice ferrimagnet are reduced to a simpler model in the basic exchange approximation, which correctly takes into account the main interactions and, at the same time, admits an analytical description by the method of inverse scattering problem [9]. In unbounded ferrimagnets, quasi-one-dimensional solitons are constructed and analyzed in detail in Refs. [9–11].

Particle-like excitations in finite-size magnets are still poorly understood because of the essential nonlinearity of the basic equations and the lack of developed methods for their integration. We have been able to apply the inverse scattering problem method to study the nonlinear dynamics of semi-bounded single-sublattice ferromagnets with different types of bulk crystallographic anisotropy and unidirectional surface anisotropy due to film coating [12–15]. It is found that the magnetization in the nuclei of ferromagnetic solitons during their interaction with the sample boundary changes by an order of saturation magnetization, and this determines the remagnetization of the surface layers of the sample. In addition, solitons acquire dynamical properties that are absent in an infinite medium and are interesting for applications.

In this paper, we study the peculiarities of nonlinear dynamics of solitons in a semi-bounded two-sublattice ferrimagnet with free edge spins. The dependence of the ferrimagnetic energy on the magnetization distribution has the following form in the exchange approximation [16]:

$$W = \int d^3\mathbf{r}\Big(\frac{1}{2}\sum_{i=1}^{3}\big[\alpha_1(\partial_i\mathbf{M}_1\,\partial_i\mathbf{M}_1) + \alpha_2(\partial_i\mathbf{M}_2\,\partial_i\mathbf{M}_2) + 2\alpha_3(\partial_i\mathbf{M}_1\,\partial_i\mathbf{M}_2)\big] + \eta(\mathbf{M}_1\mathbf{M}_2)\Big),$$

where $\eta > 0$ is the homogeneous exchange constant between sublattices, α_s is the inhomogeneous exchange constants $(s = 1, 2, 3)$, $\alpha_1 + \alpha_2 - 2\alpha_3 > 0$. By order of magnitude $\alpha_s \propto \eta a^2$, where a is the lattice constant.

Instead of sublattice magnetization, we introduce normalized ferro- and antiferromagnetism vectors:

$$\mathbf{m} = \frac{\mathbf{M}_1 + \mathbf{M}_2}{\sqrt{2(M_{01}^2 + M_{02}^2)}}, \quad \mathbf{l} = \frac{\mathbf{M}_1 - \mathbf{M}_2}{\sqrt{2(M_{01}^2 + M_{02}^2)}}.$$

They satisfy the constraints:

$$\mathbf{m}^2 + \mathbf{l}^2 = 1, \quad (\mathbf{m}\cdot\mathbf{l}) = \frac{M_{01}^2 - M_{02}^2}{2(M_{01}^2 + M_{02}^2)}.$$

The evolution equations for the vectors $\mathbf{m}$ and $\mathbf{l}$ follow from the Landau–Lifshitz equations [17–20] for the sublattice magnetizations [3,17,21]:

$$\partial_t\mathbf{M}_\nu = \gamma_\nu\left[\mathbf{M}_\nu \times \frac{\delta W}{\delta \mathbf{M}_\nu}\right], \quad \mathbf{M}_\nu^2 = M_{0\nu}^2, \quad \nu = 1, 2. \quad (1)$$

where γ_ν is the magnetomechanical ratio for the ν-th sublattice. Let us assume that the characteristic size of the magnetic inhomogeneities λ (spin wavelength, soliton size) is much larger than the lattice constant: $\lambda \gg a$. Furthermore, assuming $\mathbf{m}^2 \ll \mathbf{l}^2$, we will assume that the length of the vector $\mathbf{l}$ does not change: $\mathbf{l}^2 = 1$. Then the vector $\mathbf{m}$ can be expressed through $\mathbf{l}$ from equations (1) in the main small parameter approximation a/λ [9–11]:

$$\mathbf{m} = -\sqrt{\frac{2}{M_{01}^2 + M_{02}^2}}\,\frac{[\mathbf{l}\times\partial_t\mathbf{l}]}{\eta(\gamma_1+\gamma_2)} + \frac{M_{01}^2 - M_{02}^2}{2(M_{01}^2 + M_{02}^2)}\,\mathbf{l} + \frac{\gamma_1(\alpha_3-\alpha_1) + \gamma_2(\alpha_2-\alpha_3)}{2\eta(\gamma_1+\gamma_2)}\,\big[\mathbf{l}\times[\mathbf{l}\times\hat{\Delta}\mathbf{l}]\big], \quad (2)$$

and we obtain the closed equation for the vector $\mathbf{l}$:

$$[\mathbf{l}\times(c^{-2}\partial_t^2\mathbf{l} - \hat{\Delta}\mathbf{l})] + \beta c^{-1}\partial_t\mathbf{l} = 0, \quad \mathbf{l}^2 = 1, \quad (3)$$

where $\hat{\Delta} = \partial_x^2 + \partial_y^2 + \partial_z^2$ is the Laplace operator,

$$c^2 = \frac{1}{2}(M_{01}^2 + M_{02}^2)\eta\gamma_1\gamma_2(\alpha_1 + \alpha_2 - 2\alpha_3).$$

$$\beta = \sqrt{\frac{\eta}{\gamma_1\gamma_2(\alpha_1+\alpha_2-2\alpha_3)}} \times\left[\left(\frac{M_{02}^2 - M_{01}^2}{M_{01}^2 + M_{02}^2}\right)\frac{(\gamma_1+\gamma_2)}{2} + \gamma_1 - \gamma_2\right].$$

In the formal limit $c \to \infty$ $(\beta c^{-1} = \text{const})$, which corresponds to a tight coupling between the sublattices $(\eta \to \infty)$, the effective equation (3) coincides with the Landau–Lifshitz equation of the Heisenberg ferromagnet [17,18]. The system (2), (3) describes waves in isotropic two-sublattice antiferromagnet at $M_{01} = M_{02}$, $\gamma_1 = \gamma_2$ [6,22].

Thus, the considered model of ferrimagnet (2), (3) model is the missing link between the ferro- and antiferromagnetic models.

We next consider nonlinear excitations in a semi-bounded ferrimagnet propagating along an axis Ox perpendicular to the boundary $x = 0$ of the sample. In this case, $\mathbf{l} = \mathbf{l}(x, t)$. After scale transformations: $x \to x/\beta$, $t \to t/c\beta$, the equation for calculating $\mathbf{l}$ will look as follows:

$$[\mathbf{l}\times(\partial_t^2\mathbf{l} - \partial_x^2\mathbf{l})] + \partial_t\mathbf{l} = 0, \quad \mathbf{l}^2 = 1, \quad (4)$$

where $0 < x < \infty$, $t > 0$.

The choice of solutions is defined by the boundary conditions:

$$[\mathbf{l}\times\partial_x\mathbf{l}]\big|_{x=0} = 0; \quad (5)$$

$$\partial_t\mathbf{l},\ \partial_x\mathbf{l} \to 0, \quad \mathbf{l} \to (0, 0, 1) \text{ by } x \to \infty \quad (6)$$

and initial conditions:

$$\partial_t\mathbf{l}(x, t=0) = \partial_t\mathbf{l}_0(x),\ \mathbf{l}(x, t=0) = \mathbf{l}_0(x),\ 0 < x < \infty. \quad (7)$$

The relation (5) corresponds to the absence of spin anchoring on the surface $x = 0$ of the sample [21]. The

second condition (6) corresponds to the minimum of the energy density of the medium:

$$w = \frac{1}{2}\left[(\partial_x \mathbf{l})^2 + (\partial_t \mathbf{l})^2\right]$$

in the depth of the sample. The initial distribution of the vector field $\mathbf{l}(x, t)$ (7) should be consistent with the boundary conditions (5), (6). We will show in Section 2 that the initial-boundary value problem (4)–(7) can be extended by a certain symmetry from the semi-axis $0 < x < \infty$ to the entire axis $-\infty < x < \infty$. Then its solution is obtained by a special modification of the method for the inverse scattering problem on the interval $-\infty < x < \infty$. The procedure constitutes a nonlinear generalization of the „image method" used in electrostatics to solve linear boundary value problems with certain spatial symmetry.

In the context of the inverse scattering problem method, an auxiliary system of linear differential equations is compared to the essentially nonlinear model (4)–(7). Transformation, analytical and asymptotic properties of its solutions are determined in Section 2. Spectral expansions of the integrals of motion of a semi-bounded sample are obtained on this basis in Section 3 and it is shown that any initial perturbation of a ferrimagnet can be described in terms of an ideal gas of solitons and magnons.

The spectral data of an auxiliary linear system are used in Section 4 to recover solutions to the original nonlinear initial boundary value problem for a ferrimagnetic.

Explicit solutions are constructed in Section 5 for the particle-like solitons of a semi-bounded ferromagnet. Their dynamical properties and features of interaction with the sample surface are analyzed.

2. „Image method" and direct scattering problem

For further analysis, let us recall some facts related to the integration of the ferrimagnetic equation:

$$\left[\mathbf{n} \times (\partial_t^2 \mathbf{n} - \partial_x^2 \mathbf{n})\right] + \partial_t \mathbf{n} = 0, \ \mathbf{n}^2 = 1, \tag{8}$$

on the interval $-\infty < x < \infty$ with asymptotic behavior:

$$\partial_t \mathbf{n}, \ \partial_x \mathbf{n} \to 0, \quad \mathbf{n} \to (0, 0, 1) \text{ by } |x| \to \infty \tag{9}$$

and initial conditions:

$$\partial_t \mathbf{n}(x, t = 0) = \partial_t \mathbf{n}_0(x), \quad \mathbf{n}(x, t = 0) = \mathbf{n}_0(x), \quad -\infty < x < +\infty. \tag{10}$$

When the vector function $\mathbf{n}(x, t)$ is differentiable on the variables x and t the nonlinear equation (8) is equivalent to the compatibility condition:

$$\left[\partial_x - U(u), \ \partial_t - V(u)\right] = 0 \tag{11}$$

of the system of linear differential equations:

$$\partial_x \Psi = U(u)\Psi, \quad \partial_t \Psi = V(u)\Psi - i(\gamma^2/2)\Psi\sigma_3 \tag{12}$$

for auxiliary matrix functions $\Psi(x, t, u)$. The operators U and V look as follows:

$$U = -\frac{i}{2}\left(\gamma[\mathbf{n} \times \partial_t \mathbf{n}]_a + \delta[\mathbf{n} \times \partial_x \mathbf{n}]_a + \Lambda n_a\right)\sigma_a,$$

$$V = -\frac{i}{2}\left(\delta[\mathbf{n} \times \partial_t \mathbf{n}]_a + \gamma[\mathbf{n} \times \partial_x \mathbf{n}]_a - \gamma^2 n_a\right)\sigma_a, \tag{13}$$

where σ_a are the Pauli matrices, the indices occurring twice imply summation ($a = 1, 2, 3$). The coefficients γ, δ, Λ are related by algebraic equations:

$$(\delta - 1)^2 - \gamma^2 = 1, \quad \Lambda = \gamma(1 - \delta). \tag{14}$$

The uniformization of relations (14) by rational functions of the spectral parameter u was used in Ref. [9,11]. A different parameterization is introduced in this paper to simplify the formulas:

$$\delta = 1 - \coth u, \quad \gamma = -\sinh^{-1} u, \quad \Lambda = -\cosh u \sinh^{-2} u.$$

Therefore, the domain of definition of the parameter u will be the surface of the cylinder:

$$u = \rho + i\varphi, \ -\infty < \rho < +\infty, \ -\pi < \varphi \leq \pi \ (\mathrm{mod}\, 2\pi). \tag{15}$$

To incorporate the initial boundary value problem (4)–(7) into the scheme of the inverse scattering problem, let us extend the field $\mathbf{l}(x, t)$ in an even manner over the whole interval $-\infty < x < +\infty$:

$$\mathbf{n}(x, t) = \begin{cases} \mathbf{l}(x, t), & 0 \leq x < \infty, \\ \mathbf{l}(-x, t), & -\infty < x < 0. \end{cases} \tag{16}$$

The extension is continuous at the point $x = 0$:

$$\mathbf{n}(-0, t) = \mathbf{n}(+0, t) = \mathbf{l}(+0, t),$$

but its first derivative at the point $x = 0$ has a jump:

$$\partial_x \mathbf{n}\big|_{x=+0} - \partial_x \mathbf{n}\big|_{x=-0} = 2\partial_x \mathbf{l}\big|_{x=+0}.$$

This fact allows treating the boundary condition (5) for $\mathbf{l}(x, t)$ at $x = 0$ as an additional constraint on the choice of the vector function $\mathbf{n}(x, t)$:

$$\Delta\mathbf{n}\big|_{x=0} = 0, \quad [\mathbf{n} \times \Delta\partial_x \mathbf{n}]\big|_{x=0} = 0, \tag{17}$$

where $\Delta f\big|_{x=0} = f(x = +0) - f(x = -0)$. Importantly, the commutation representation (11) is equivalent to equation (8) for calculation of the field $\mathbf{n}(x, t)$ at $x \neq 0$ and the additional constraint (17) at $x = 0$. This allows including the problem for the ferrimagnetic on the semi-axis (4)–(7) in the traditional scheme of the method for the inverse scattering problem on the entire axis $-\infty < x < +\infty$ [11]. The derivatives $\partial_x \Psi$ and $\partial_t \Psi$ in equations (12) are continuous at the point $x = 0$ with the constraint (17).

It is necessary to analyze the solutions of the auxiliary linear system (12) for integrating the nonlinear

model (8)–(10), (16), (17). Let us introduce the fundamental Jost solutions of the matrix equation:

$$\partial_x \Psi_\pm = U\Psi_\pm \tag{18}$$

with asymptotic boundary conditions:

$$\Psi_\pm \to \exp\left(-\frac{i\Lambda}{2}x\sigma_3\right) \text{ by } x \to \pm\infty, \tag{19}$$

which are consistent with the field behavior $\mathbf{l}(x,t)$ at $x \to +\infty$. It should be noted that the last term in the right-hand side of the second equation (12) is introduced to preserve the condition (19) at all values t. In view of the tracelessness of the matrix U, we conclude from (18), (19), that

$$\det \Psi_\pm = 1. \tag{20}$$

On the set

$$\Gamma = \{u \,|\, 0 < \rho < +\infty, \varphi = 0, \pi; -\infty < \rho < 0, \varphi = 0, -\pi; \\ \rho = 0, -\pi < \varphi < \pi\} \tag{21}$$

when $x \to \pm\infty$ the Jost functions oscillate. Therefore Γ corresponds to the continuous spectrum of the scattering problem (18), (19).

Two sets of basis solutions are connected on the contour Γ:

$$\Psi_-(x,t,u) = \Psi_+(x,t,u)T(u,t), \quad u \in \Gamma. \tag{22}$$

The transition matrix T depends only on the spectral parameter u and time t. To simplify the formulas, we further omit the dependence on t where it is not confusing.

As in the unbounded environment [9,11], the matrix solutions satisfy involutions:

$$\sigma_2 \Psi_\pm^*(u^*)\sigma_2 = \Psi_\pm(u), \quad n_a \sigma_a \Psi_\pm(-u) = \Psi_\pm(u)\sigma_3. \tag{23}$$

The parity of continuation (16) gives rise to a restriction on the choice of Jost functions [13–15]:

$$\Psi_+(x,u) = \sigma_2 \Psi_-^*(-x, u^* \pm \pi i)\sigma_2. \tag{24}$$

Next, we will number the columns of matrices 2×2 with upper indices: $\Psi = (\Psi^{(1)}, \Psi^{(2)})$. The vector functions $\Psi_-^{(1)}(u)$ and $\Psi_+^{(2)}(u)$ continue analytically from the contour Γ into the region D_1 (see Figure 1):

$$D_1 = \{u | 0 < \rho < \infty, 0 < \varphi < \pi; -\infty < \rho < 0, -\pi < \varphi < 0\},$$

and the columns $\Psi_+^{(1)}(u)$ and $\Psi_-^{(2)}(u)$ will be analytical functions in the region D_2:

$$D_2 = \{u | 0 < \rho < \infty, -\pi < \varphi < 0; -\infty < \rho < 0, 0 < \varphi < \pi\}.$$

The traversal of the contour lines Γ is chosen so in Figure 1 that the region D_1 remains to the left of contour Γ.

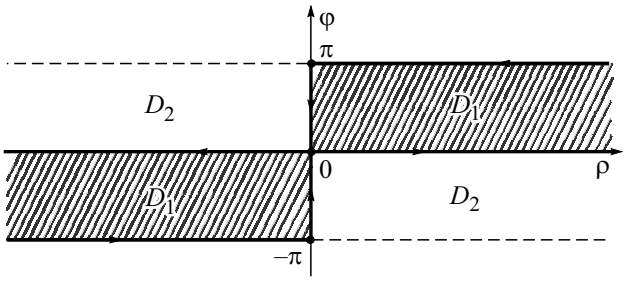

Figure 1. The analyticity regions D_1 of functions $\Psi_-^{(1)}(u)$, $\Psi_+^{(2)}(u)$, $a(u)$ and D_2 functions $\Psi_+^{(1)}(u)$, $\Psi_-^{(1)}(u)$, $\bar{a}(u)$ on the surface of a cylinder. The contour Γ is represented by a thick line.

The reductions (23), (24) can be continued from the contour Γ in the analyticity region of the corresponding columns of the Jost matrices. They concretize the form of the transition matrix:

$$T(u) = \begin{pmatrix} a(u) & -\bar{b}(u) \\ b(u) & \bar{a}(u) \end{pmatrix}, \; a(u)\bar{a}(u) + b(u)\bar{b}(u) = 1,$$

$$\bar{a}(u) = a^*(u^*), \quad \bar{b}(u) = b^*(u^*);$$

$$a(u) = a(-u) = a^*[(u + \pi i)^*], \quad u \in D_1;$$

$$b(u) = -b(-u) = b^*[(u + \pi i)^*], \quad u \in \Gamma. \tag{25}$$

Here we have considered that the matrix elements $a(u)$ and $\bar{a}(u)$ admit representations [11]:

$$a(u) = \det\left(\Psi_-^{(1)}(u), \Psi_+^{(2)}(u)\right), \; \bar{a}(u) = \det\left(\Psi_+^{(1)}(u), \Psi_-^{(2)}(u)\right), \tag{26}$$

and thus can be analytically extended from the contour Γ to the regions D_1 and D_2, respectively. The reflection coefficients $b(u)$ and $\bar{b}(u)$ are determined only on Γ.

The matrix elements $a(u)$ and $\bar{a}(u)$ may have zeros in their analyticity regions, which we will assume to be simple. If $u = u_j \in D_1$ is zero of the function $a(u)$, then $u = u_j^* \in D_2$ will be zero of the function $\bar{a}(u)$. As in [14], the reductions (23), (24) combine zeros of the coefficient $a(u)$ into „quartets“:

$$u = \mu_k, \; -\mu_k, \; \mu_k^* + \pi i, \; -\mu_k^* - \pi i, \; k = 1, 2, \ldots, N;$$

$$\mu_k = \tau_k + i\left(\frac{\pi}{2} + \varepsilon_k\right), \; 0 < \tau_k < \infty, \; -\frac{\pi}{2} < \varepsilon_k < \frac{\pi}{2}. \tag{27}$$

According to (26), if $a(u_j) = 0$, then the columns $\Psi_-^{(1)}(u_j)$ and $\Psi_+^{(2)}(u_j)$ are proportional:

$$\Psi_-^{(1)}(u_j) = c(u_j)\Psi_+^{(2)}(u_j). \tag{28}$$

The formulas (28) define the vector solutions of the system (18), which are exponentially decreasing when $|x| \to \infty$. Therefore, the set $\{u_j\}$ corresponds to the discrete spectrum of the scattering problem (18), (19).

Reductions to Jost solutions (23), (24) define the choice of multipliers $c(u_j)$ for each group of zeros (27):

$$c(\mu_k),\ \ c(-\mu_k) = -c(\mu_k),\ \ c(\mu_k^* + \pi i) = -\frac{1}{c^*(\mu_k)}.$$

$$c(-\mu_k^* - \pi i) = \frac{1}{c^*(\mu_k)}, \quad k = 1, 2, \ldots, N. \tag{29}$$

Since the functions $\Psi_\pm(u)$ are continuous at the point $x = 0$, there is a useful representation of the transition matrix:

$$T(u) = \Psi_+^{-1}(x = 0, u)\Psi_-(x = 0, u).$$

From here, in particular, we find:

$$a(u) = [\Psi_+(0, u)]_{22}[\Psi_-(0, u)]_{11} - [\Psi_+(0, u)]_{12}[\Psi_-(0, u)]_{21}. \tag{30}$$

For further analysis, we need asymptotic expansions of the functions $\Psi_\pm(u)$ near the singular point $u = 0$ of equation (18). Let $x > 0$ for definiteness. Let's represent $\Psi_+(u)$ in the following form:

$$\Psi_+(u) = [I + \Phi(x, u)] \exp\left(-\frac{i}{2}\Lambda(u)x\sigma_3 + Z(u, x)\right), \tag{31}$$

where Φ and Z are the antidiagonal and diagonal matrix functions such that

$$\Phi, Z \to 0 \quad \text{by} \quad x \to +\infty.$$

The special symmetry of the operator U in equation (18) allows concluding that

$$\Phi = \begin{pmatrix} 0 & -\omega^* \\ \omega & 0 \end{pmatrix}, \quad Z = \begin{pmatrix} \xi & 0 \\ 0 & \xi^* \end{pmatrix}. \tag{32}$$

After substituting the expressions (31), (32) into (18) and separating the diagonal and non-diagonal parts, we obtain a system for calculating the functions $\omega(x, u)$, $\xi(x, u)$:

$$\partial_x\xi = \frac{i\Lambda}{2} + U_{11} + U_{12}\omega,\ \ \partial_x\omega + 2\omega U_{11} + \omega U_{12}\omega - U_{21} = 0. \tag{33}$$

Let us decompose the coefficients of γ, δ, Λ into series by powers of u:

$$\gamma = -\frac{1}{u} + \sum_{k=0}^{\infty} u^{2k+1}\gamma_{2k+1},\ \ \delta = -\frac{1}{u} + 1 + \sum_{k=0}^{\infty} u^{2k+1}\delta_{2k+1}.$$

$$\Lambda = -\frac{1}{u^2} - \frac{1}{6} + \sum_{k=1}^{\infty} u^{2k}\Lambda_{2k}.$$

We will look for functions $\omega(x, u)$, $\xi(x, u)$ in the following form:

$$\omega = \sum_{k=0}^{\infty} \omega_k u^k, \quad \xi = \sum_{k=0}^{\infty} \xi_k u^k. \tag{34}$$

Then the system (33) gives a chain of equations for recurrently determining the coefficients $\omega_k(x)$, $\xi_k(x)$. The computation is simplified in the parameterization of the unit vector $\mathbf{l}$ by the angles Θ, Φ:

$$\mathbf{l} = (\sin\Theta\cos\Phi, \sin\Theta\sin\Phi, \cos\Theta). \tag{35}$$

Here are the expressions for the first coefficients:

$$\omega^{(0)} = \tan\frac{\Theta}{2}\exp(i\Phi),$$

$$\xi^{(0)} = -\frac{i}{4}\int_x^{+\infty} dx' \Big[(\partial_{x'}\Theta + \partial_t\Theta)^2 + \sin^2\Theta(\partial_{x'}\Phi + \partial_t\Phi)^2$$

$$+ 2(\cos\Theta - 1)\partial_{x'}\Phi\Big] + \ln\cos\frac{\Theta}{2}. \tag{36}$$

The expansion of the function $\Psi_-(u)$ at $x < 0$ by powers of u is obtained from that for the function $\Psi_+(u)$ at $x > 0$ by formal substitution:

$$\mathbf{l}(x) \to \mathbf{l}(-x), \quad \int_x^{+\infty} dx' \to \int_x^{-\infty} dx'. \tag{37}$$

The formulas (18), (19) lead to the relation:

$$\Psi_+(\mathrm{Re}\, u \to +\infty) \to I, \tag{38}$$

where I is a unit matrix. Then we obtain from the representation (30):

$$a(\mathrm{Re}\, u \to +\infty) = 1. \tag{39}$$

The explicit form of the analytical function $a(u)$ is recovered from its zeros (27) in the region D_1, the asymptotic behavior (39), and the reflection coefficient [11]:

$$a(u) = \prod_{k=1}^{N}\left(\frac{\cosh u - \cosh\mu_k}{\cosh u - \cosh\mu_k^*}\right)\left(\frac{\cosh u + \cosh\mu_k^*}{\cosh u + \cosh\mu_k}\right)$$

$$\times\exp\left[\frac{1}{2\pi i}\int_0^{\infty} d\nu \ln(1 - |b(\nu)|^2)\left(\frac{1}{\sinh(\nu - u)} + \frac{1}{\sinh(\nu + u)}\right)\right]$$

$$\times\exp\left[-\frac{1}{2\pi i}\int_0^{\pi} d\varphi \ln(1 + |b(i\varphi)|^2)\,\frac{\sin\varphi}{(\cosh u - \cos\varphi)}\right]. \tag{40}$$

Here we have used the Cauchy kernel on the surface of the cylinder $(\exp u' - \exp u)^{-1}\exp u'$ [23] and the symmetry properties of the functions $a(u)$ and $b(u)$ (25).

Thus, using the auxiliary linear system (18), we have mapped the vector field $\mathbf{l}(x, t)$ of the semi-bounded ferrimagnet into the scattering data set. It contains the spectral densities $b(\lambda)$ ($\lambda \in \Gamma$) of the scattering problem (18), (19), the discrete zeros $\{u_j\}$ of functions $a(u)$, and the normalized coefficients $\{c(u_j)\}$. The evolution of the scattering data is found using the standard method [11] by means of the second equation (12):

$$b(u, t) = b_0(u)\exp[-i\gamma^2(u)t],$$

$$c(u_j, t) = c_0(u_j)\exp[-i\gamma^2(u_j)t],\ \ a(u,t) = a_0(u). \quad (41)$$

The integration constants $b_0(u)$, $c_0(u_j)$, $a_0(u)$ are determined from equation (18) by the given initial condition (10) at $t = 0$.

The described scheme represents a nonlinear generalization of the Fourier method, which is widely used in the analysis of small-amplitude spin waves. For weakly excited states of the medium, the spectral densities $b(u,t)$ of the scattering problem are exactly the same as the Fourier harmonics of the linear modes of the ferrimagnetic. In general case, the $b(u,t)$ functions describe the weakly nonlinear dynamics of dispersive wave trains. Data of the discrete spectrum $\{u_j\}$ parameterize particle-like normal modes — solitons, which form only under strong external forcing and have no analogues in linear theory.

3. Integrals of the motion of a semi-infinite ferrimagnet

As in the unbounded medium, the time-independent element $a(u)$ of the transition matrix serves as the derivative function of an infinite series of motion integrals for a nonlinear dynamics of the semi-infinite ferrimagnet. Physically meaningful local integrals of motion coincide with the coefficients of the expansion of the function $\ln a(u)$ in a series by powers u. It is not difficult to obtain it by using the formulas (30)–(37) of the previous section.

Let us give the first term of the power series:

$$\ln a(u) = iE + O(u).$$

It coincides with the energy of the semi-bounded sample:

$$E = \frac{1}{2}\int_0^{+\infty} dx\left[(\partial_t\Theta)^2 + (\partial_x\Theta)^2 + \sin^2\Theta[(\partial_x\Phi)^2 + (\partial_t\Phi)^2]\right]$$

$$= \frac{1}{2}\int_0^{+\infty} dx\left[(\partial_x\mathbf{l})^2 + (\partial_t\mathbf{l})^2\right].$$

On the other hand, we obtain the dispersion relation (40) for the function $a(u)$. It can also be written as a series of powers u. Comparing the two expansions allows expressing all integrals of motion in terms of spectral data. In particular, the energy of a semi-infinite ferrimagnet admits the following representation:

$$E = \int_0^{\infty} d\rho N_G(\rho)\omega_G(\rho) + \int_0^{\pi} d\varphi N_a(\varphi)\omega_a(\varphi)$$

$$+ 4\sum_{k=1}^{N}\arctan\left(\frac{\cos\theta_k}{\sinh\tau_k}\right), \quad (42)$$

where the values

$$N_G(\rho) = -\frac{\sinh\rho}{\pi}\ln[1 - |b(\rho)|^2] > 0,$$

$$N_a(\varphi) = \frac{\sin\varphi}{2\pi}\ln[1 + |b(i\varphi)|^2] > 0$$

represents of the densities of zero-gap (Goldstone) and activation magnons with frequencies

$$\omega_G(\rho) = \sinh^{-2}\rho, \quad \omega_a(\varphi) = \sin^{-2}\varphi. \quad (43)$$

Let us justify this statement by proceeding from the parameters ρ and φ to the quasi-momentums p_G and p_a of magnons [11]:

$$p_G^2 = \frac{\cosh^2\rho}{\sinh^4\rho}, \quad p_a^2 = \frac{\cos^2\varphi}{\sin^4\varphi}. \quad (44)$$

Then the formulas (43), (44) will exactly coincide with the laws of dispersion of linear modes of ferrimagnetic [11]:

$$\omega_G(\rho) = \frac{1}{2}\left[\sqrt{1 + 4p_G^2} - 1\right],\ \ \omega_a(\rho) = \frac{1}{2}\left[\sqrt{1 + 4p_a^2} + 1\right].$$

The discrete terms in representation (42) correspond to the contributions to the sample energy of individual solitons.

Hence we conclude that any nonlinear excitation of a semi-bounded ferrimagnet can be described in terms of an ideal gas of discrete essentially nonlinear modes — solitons, and quasiparticles of a continuous spectrum of dispersive waves — magnons.

4. Inverse spectral transformation

To solve the original initial boundary value problem (4)–(7) for a ferrimagnetic, we need to find the inverse transformation of the scattering data (41) into the vector field $\mathbf{l}(x,t)$. With this purpose, we first construct the solution of the auxiliary linear system (12).

Let us proceed from the Jost matrices to the new fundamental solutions $\Pi_+(u)$ and $\Pi_-(u)$ of the system (12):

$$\Pi_+(u) = \left(\Psi_-^{(1)}(u), \Psi_+^{(2)}(u)\right)\varphi_0^{-1}(u),$$

$$\Pi_-(u) = \left(\Psi_+^{(1)}(u), \Psi_-^{(2)}(u)\right)\varphi_0^{-1}(u), \quad (45)$$

where $\varphi_0(u) = \exp[-i\Lambda(u)x\sigma_3/2]$. According to the results of Section 3, $\Pi_+(u)$ and $\Pi_-(u)$ will be analytical functions of the parameter u in the regions of D_1 and D_2, respectively. Therefore, the problem of their computation is reduced to solving the following Riemann problem of the theory of functions of a complex variable. We need to construct matrix functions $\Pi_+(x,u)$ and $\Pi_-(x,u)$, analytical with respect to u in the regions analytical with respect to u in the regions ¡.¿, which are connected by the conjugacy condition, which are connected by the conjugacy condition on the contour Γ:

$$\Pi_-(x,u) = \frac{\Pi_+(x,u)}{a(u)}\varphi_0(x,u)$$

$$\times\begin{pmatrix} 1 & -\bar{b}(u) \\ -b(u) & 1 \end{pmatrix}\varphi_0^{-1}(x,u), \quad (46)$$

satisfy the constraints:

$$n_a(x)\sigma_a\Pi_\pm(x,u)=\Pi_\pm(x,-u)\sigma_3, \tag{47}$$

$$\Pi_\pm(x,u)=\sigma_2\Pi_\pm^*\big(-x,(u+\pi i)^*\big)\sigma_2,\quad u\in D_{1,2};$$
$$\Pi_+^*(x,u)=\sigma_2\Pi_-(x,u)\sigma_2,\quad u\in\Gamma \tag{48}$$

and the normalization condition:

$$\Pi_\pm(x,u=+\infty)=I. \tag{49}$$

The Riemann problem (46)–(49) is a reformulation of the analytical and transformation properties of the Jost basis functions of Section 3 and their connection (22) on contour Γ.

The following equality is true for any nondegenerate matrix A of order 2×2:

$$A^{-1}\det A=\sigma_2 A^T\sigma_2.$$

Therefore, equality (48) can be reduced to the following form:

$$\Pi_+^{-1}(x,u)a(u)=\Pi_-^\dagger(x,u^*).$$

Here, the upper indices „T“ and † denote the transpose and Hermitian conjugation operations. This allows rewriting the conjugacy condition (46) in terms of the function $\Pi_-(x,u)$ alone:

$$\Pi_-^\dagger(x,u^*)\Pi_-(x,u)=\varphi_0(x,u)\times\begin{pmatrix}1 & -\bar b(u)\\ -b(u) & 1\end{pmatrix}\varphi_0^{-1}(x,u),\ u\in\Gamma. \tag{50}$$

At large times, weakly nonlinear waves become blurred due to dispersion effects and only long-lived solitons „survive“. They determine the basic physical properties of a ferrimagnet under strong external influences. Therefore, in what follows, we will limit our discussion to purely soliton states, where there are no dispersive waves. Then $b(u)=\bar b(u)\equiv 0$, and the conjugacy condition (50) is simplified:

$$\Pi_-^\dagger(x,u^*)\Pi_-(x,u)=\Pi_-(x,u)\Pi_-^\dagger(x,u^*)=I,\ u\in\Gamma. \tag{51}$$

The Riemann problem is reduced to constructing a matrix function $\Pi_-(u)$ meromorphic on the surface of the cylinder (15) with poles at points $u=u_j\in D_1$ (27) and normalization condition (49). We'll look for it in the following form:

$$\Pi_-(u)=I+\sum_{j=1}^{4N}\frac{A_j}{\exp u-\exp u_j}. \tag{52}$$

The condition of absence of poles in the left-hand side of equality (51) leads to $4N$ independent matrix equations [11,24]:

$$\Pi_-(u_j^*)A_j^+=0,\quad j=1,2,\ldots,4N. \tag{53}$$

Their nontrivial solution is possible only when both matrices A_j and $\Pi_-(u_j^*)$ are degenerate. Let us represent A_j in the following form [24]:

$$(A_j)_{\alpha\beta}=(X_j)_\alpha(\xi_j^*)_\beta,\quad \alpha,\beta=1,2.$$

Then equations (53) will have the form:

$$\Pi_-(u_j^*)\xi_j=0,\quad j=1,2,\ldots,4N. \tag{54}$$

The formulas of the previous section reveal the algebraic structure of the matrix $\Pi_-(u_j^*)$ when $x>0$ [12–15]:

$$\Pi_-(u_j^*)=i\sigma_2\Big(\Psi_+^{(2)}(u_j),-c^*(u_j)\Psi_+^{(2)}(u_j)\Big)\varphi_0^{-1}(u_j^*).$$

From here, we immediately find the vectors ξ_j up to the irrelevant common multiplier:

$$\xi_j=\begin{pmatrix}\nu_j^*(x,t)\\ 1\end{pmatrix},$$
$$\nu_j(x,t)=c_0(u_j)\exp\big[-i\big(\gamma^2(u_j)t-\Lambda(u_j)x\big)\big], \tag{55}$$

where $c_0(u_j)$ are the integration constants in formulas (41). Here we have recovered the dependence on time.

We would like to remind that discrete spectrum data are combined into „quartets“:

$$\{u_j\}\equiv\{u_k^{(1,2)},u_k^{(3,4)}\},\quad \{c_0(u_j)\}=\{c_k^{(1,2)},c_k^{(3,4)}\},$$
$$j=1,2,\ldots,4N,\quad k=1,2,\ldots,N.$$

Within each group the parameters are related to each other:

$$u_k^{(1,2)}=\pm\mu_k,\ u_k^{(3,4)}=\pm(\mu_k^*+\pi i),\ \mu_k=\tau_k+i\left(\frac{\pi}{2}+\varepsilon_k\right),$$
$$0<\tau_k<\infty,\quad -\pi/2<\varepsilon_k<\pi/2;$$
$$c_k^{(1,2)}=\pm c_k^{(0)},\quad c_k^{(3,4)}=\mp(c_k^{(0)^*})^{-1}. \tag{56}$$

Here $c_k^{(0)}=c^{(0)}(\mu_k)$ is the complex integration constant.

Substituting ξ_j (55) into (54) results in a linear system for calculating the vectors X_j:

$$\xi_j+\sum_{k=1}^{4N}M_{jk}X_k=0,\quad M_{jk}=\frac{(\xi_k^*\cdot\xi_j)}{\exp u_j^*-\exp u_k}.$$

Its solution determines the soliton matrix $\Pi_-(x,t,u)$ at $x>0$:

$$(\Pi_-)_{\alpha\beta}=\delta_{\alpha\beta}-\sum_{k,j=1}^{4N}\frac{(M^{-1})_{kj}(\xi_i)_\alpha(\xi_k^*)_\beta}{\exp u-\exp u_k}$$
$$(M^{-1})_{kj}=\frac{\partial\ln\det M}{\partial M_{jk}}. \tag{57}$$

Then the first formula (47) with the normalization condition (49) and the explicit form of the matrix function $\Pi_-(u)$ at $x>0$ (57) immediately gives N–soliton solution of the original essentially nonlinear model (4)–(6) for the ferrimagnet on the semi-axis $0<x<\infty$:

$$l_a\sigma_a=\Pi(u=-\infty)\sigma_3. \tag{58}$$

It describes elastic pairwise collisions of solitons with each other and their reflection from the sample boundary.

5. Interaction of solitons with the surface of a ferrimagnet

Let us analyze the typical features of multisoliton interaction on the example, of a single-soliton solution that is parameterized by four zeros (56) of function $a(u)$:

$$u^{(1,2)} = \pm\mu, \quad u^{(3,4)} = \pm(\mu^* + \pi i), \quad \mu = \tau + i\left(\frac{\pi}{2} + \varepsilon\right),$$

$$0 < \tau < \infty, \quad |\varepsilon| < \frac{\pi}{2}.$$

The corresponding vectors ξ_j (55) have the form:

$$\xi_{1,2} = \begin{pmatrix} \pm\nu_1^* \\ 1 \end{pmatrix}, \quad \xi_{3,2} = \begin{pmatrix} \pm\nu_3^* \\ 1 \end{pmatrix}.$$

The field distribution of $\mathbf{l}(x,t)$ in single-soliton excitation is given by the formulas (57), (58) when $N = 1$. The following form of writing is convenient for further analysis:

$$l_3 = 1 - \frac{2|f|^2}{|f|^2 + |g|^2}, \quad l_1 + il_2 = \frac{2f^* g}{|f|^2 + |g|^2}. \qquad (59)$$

After simple but tedious transformations, we find the functions f and g:

$$f = i\tan\varepsilon\coth\tau\left[\nu_1^*(\nu_1\nu_3^* - 1)\tanh\mu - \nu_3^*(\nu_1^*\nu_3 - 1)\tanh\mu^*\right],$$

$$g = \frac{1}{2}\left[\left(1 + |\nu_1\nu_3|^2\right)|\tanh\mu|^2\tan^2\varepsilon\coth^2\tau\right.$$

$$\left. + |\tanh\mu|^2(\nu_1\nu_3^* + \nu_1^*\nu_3) + \frac{\sinh^2\mu|\nu_1|^2 + \sinh^2\mu^*|\nu_3|^2}{\cos^2\varepsilon\sinh^2\tau}\right]. \qquad (60)$$

Here

$$\nu_1 = c_0\exp\left[-d^{-1}(x - Vt) - ikx - i\omega t\right],$$

$$\nu_3 = -(c_0^*)^{-1}\exp\left[-d^{-1}(x + Vt) + ikx - i\omega t\right], \qquad (61)$$

c_0 — complex integration constant. Parameters d and V:

$$d = \frac{1}{\operatorname{Im}\Lambda(\mu)} = \frac{(\sinh^2\tau + \cos^2\varepsilon)^2}{\cos\varepsilon\sinh\tau\,(\cosh^2\tau + \sin^2\varepsilon)} > 0,$$

$$V = \frac{\operatorname{Im}\gamma^2(\mu)}{\operatorname{Im}\Lambda(\mu)} = \frac{2\sin\varepsilon\cosh\tau}{\cosh^2\tau + \sin^2\varepsilon}$$

determine, respectively, the size of the soliton and its velocity as a whole. The frequency ω and wave number k of the oscillations of the vector $\mathbf{l}$ inside the soliton have the form:

$$\omega = \operatorname{Re}\gamma^2(\mu) = \frac{\sin^2\varepsilon\sinh^2\tau - \cosh^2\varepsilon\cos^2\varepsilon}{(\sinh^2\tau + \cos^2\varepsilon)^2},$$

$$k = -\operatorname{Re}\Lambda(\mu) = -\frac{\cosh\tau\sin\varepsilon(\sinh^2\tau - \cos^2\varepsilon)}{(\sinh^2\tau + \cos^2\varepsilon)^2}.$$

The particle-like formation (59)–(61) satisfies the boundary conditions (5), (6) as expected. Its spatial localization and dynamical properties are determined by the exponential multipliers in formulas (61).

We assume, that the parameter $V > 0$ $(0 < \varepsilon < \pi/2)$ for definiteness. Then it is possible to put assume $\nu_3 = 0$ $(\nu_1 = 0)$ at large distances from the sample edge (at $x \gg 1$) in the limit $t \to +\infty$ $(t \to -\infty)$ in the soliton reference frame, where $x - Vt = \text{const}$ $(x + Vt = \text{const})$. In result, the formulas (59)–(61) for the vector $\mathbf{l}$ are simplified:

$$(l_3)_\pm = 1 - \frac{2}{\Delta_\pm}, \quad \Delta_\pm = \frac{\cosh^2 y_\pm}{\cos^2\varepsilon} + \frac{\sinh^2 y_\pm}{\sinh^2\tau},$$

$$(l_1 + il_2)_\pm = \frac{i\exp(-is_\pm)}{\Delta_\pm\sinh\tau\cos\varepsilon} \times \left[\sinh\mu^*\exp(\pm y_\pm) + \sinh\mu\exp(\mp y_\pm)\right], \qquad (62)$$

where

$$y_\pm = d^{-1}(x \mp Vt - x_\pm^{(0)}), \quad s_\pm = \omega t \pm kx + s_\pm^{(0)},$$

$$x_+^{(0)} = d\ln\left|\frac{c_0\cosh\mu}{\cosh\tau\sin\varepsilon}\right|, \quad x_-^{(0)} = d\ln\left|\frac{\cosh\mu}{c_0\cosh\tau\sin\varepsilon}\right|,$$

$$s_+^{(0)} = -\arg\left(\frac{\cosh\tau\sin\varepsilon}{c_0\cosh\mu}\right), \quad s_=^{(0)} = \arg\left(\frac{c_0^*\cosh\tau\sin\varepsilon}{\cosh\mu^*}\right).$$

The limit solution (62) corresponds to a typical soliton of an infinite ferrimagnet [9,11]. It can be interpreted as a bound state of two spatially localized magnetization waves propagating along the sublattices of the ferrimagnetic. Due to the sublattice non-equivalence, in the soliton formation region, the uncompensated magnetization makes an inhomogeneous circular precession around the axis Oz. A precession wave with frequency ω and wave number k nucleates at one edge of the soliton, propagates through its core, and vanishes at the opposite edge. In soliton reference frames at its center, where $y_\pm = 0$, we have:

$$(l_3)_\pm = -\cos(2\varepsilon),$$

$$(l_1 + il_2)_\pm = -i\sin(2\varepsilon)\exp\left[-i(\Omega t \pm kx_\pm^{(0)} + s_\pm^{(0)})\right]. \qquad (63)$$

Here $\Omega = \omega + kV$ is the frequency of internal precession in the soliton reference frame associated with the soliton. When $\varepsilon \to \pm\pi/2$, the deviations of the vector $\mathbf{l}$ from the equilibrium position $\mathbf{l} = (0, 0, 1)$ decrease and the soliton length increases. In this limit in the laboratory reference frame, the excitation (62) is similar to „cut off“ spin wave of linear theory with wave number $k = \mp\cosh\tau/\sinh^2\tau$ and the law of dispersion:

$$\omega(k) = \sinh^{-2}\tau = \frac{\sqrt{1 + 4k^2} - 1}{2}.$$

In the general case, the only result of the interaction of the soliton with the sample boundary as it moves away from the surface are the shift of the soliton center by the value

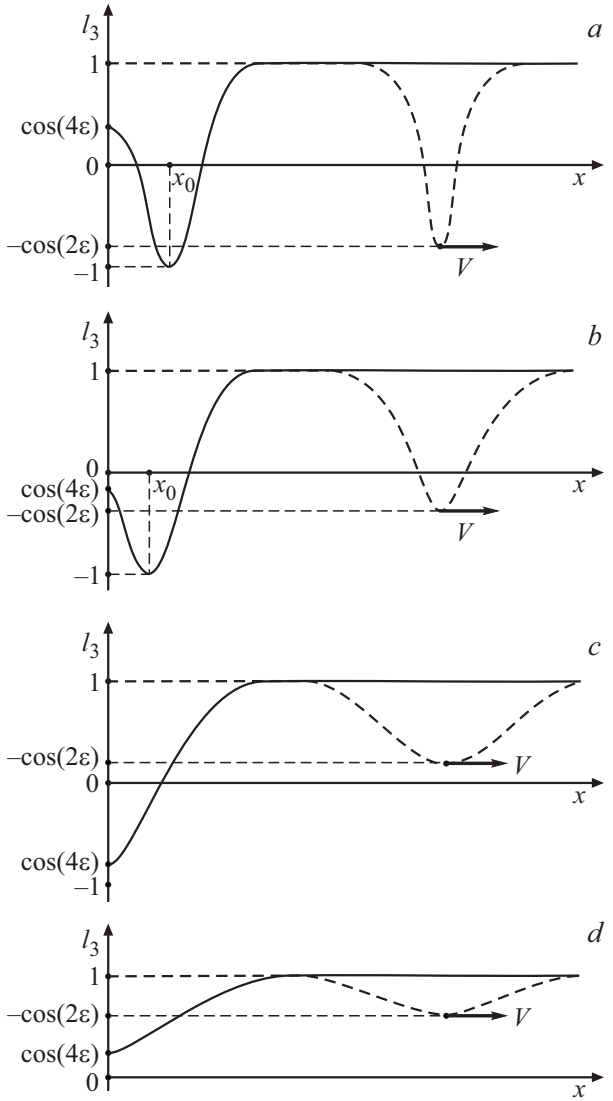

Figure 2. Dependence of the l_3 soliton component on the coordinate at the moment of collision with the sample surface (solid line) and at large distances from the surface at $V > 0$ $(0 < \varepsilon < \pi/2)$ $t \to +\infty$ (dashed line): *a*) $0 < \varepsilon \leq \pi/8$, *b*) $\pi/8 < \varepsilon \leq \pi/4$, *c*) $\pi/4 < \varepsilon \leq 3\pi/8$, *d*) $3\pi/8 < \varepsilon \leq \pi/2$.

$\Delta x = 2d \ln|c_0|$ and the change in the initial phase of its precession:

$$\Delta s = 2kd \ln\left|\frac{\cosh\mu}{\cosh\tau\,\sin\varepsilon}\right| + \arg\frac{\cosh\mu^*}{\cosh\mu}.$$

Solitons (62) can also be stationary in the depth of the sample. Their velocity is $V \to 0$ with $\varepsilon \to 0$, $x_\pm^{(0)} = \text{const}$, $s_\pm^{(0)} = \text{const}$. Meanwhile, localization of the particle-like formation (59)–(61) near the sample boundary is impossible, since, in formulas (59), (60) the multiplier f goes to zero at $\varepsilon = 0$.

When the soliton collides with the edge of the sample at time $t_0 = -(d/V)\ln|c_0|$, its center coincides with the boundary $x = 0$ of the sample, and the vector field $\mathbf{l}(x, t_0)$ on the semi-axis $0 < x < \infty$ is described by the formulas (59), where

$$g = \frac{2\exp(-2d^{-1}x)}{\sinh^2\tau + \sin^2\varepsilon}\left(\cosh^2\tau\,(\tan^2\varepsilon - 1) + (\sinh^2\tau + \cos^2\varepsilon)\right.$$
$$\left.\times\,[\sinh^2(d^{-1}x)\tan^2\varepsilon\coth^2\tau + \sin^2(kx)]\right),$$

$$f = -\frac{2i\tan\varepsilon\coth\tau\,\exp[-2d^{-1}x + i(\omega t_0 - \arg c_0)]}{\sinh^2\tau + \sin^2\varepsilon}$$
$$\times\left[\sinh(2\tau)\cos(kx)\cosh(d^{-1}x) + \sin(2\varepsilon)\sin(kx)\sinh(d^{-1}x)\right].$$

At the boundary $x = 0$ of the sample at $t = t_0$ we have:

$$l_3 = \cos(4\varepsilon),\ \ l_1 + il_2 = -i\sin(4\varepsilon)\exp[-i(\omega t - \arg c_0)]. \tag{64}$$

A comparison of the formulas (63), (64) shows that near the surface the soliton core changes thoroughly. Thus at values $\varepsilon = \pi/4$ at the center of the soliton in the depth of the sample, the component $l_3 = 0$, and at the moment of collision with the surface: $l_3 = -1$.

The processes of remagnetization of the surface layers of the material during the soliton reflection are accompanied by a boundary magnetization spike with the duration of the order of $\Delta x/V$. Scenarios for changes in the order parameter $\mathbf{l}(x, t)$ significantly depend on the values of ε (Figure 2). When $0 < |\varepsilon| < \pi/4$ at the moment of collision with the surface, the component l_3 reaches a global minimum $l_3 = -1$ near the edge of the sample at some point x_0 determined by the condition: $g(x_0, t_0) = 0$. We note, that in Figure 2, *a, b*: $\cos(4\varepsilon) = 0$ with $\varepsilon = \pi/8$; The values of $\cos(4\varepsilon)$ and $-\cos(2\varepsilon)$ coincide at $\varepsilon = \pi/6$ in Figure 2, *b*, and at $\varepsilon = \pi/4$ in Figure 2, *b, c*: $\cos(4\varepsilon) = -1$. In the interval $0 < \varepsilon < \pi/2$, the soliton size increases with the increase of ε. The extended small-amplitude soliton corresponds to Figure 2, *d*.

6. Conclusion

New soliton states of a substantially nonlinear model of a semi-bounded ferrimagnet with two crystallographically non-equivalent sublattices are found in this paper. Boundary conditions corresponding to the absence of surface spin anchoring were taken into account. It is shown that any initial excitation of a ferrimagnet can be described in terms of an ideal gas of solitons and quasiparticles of a continuous spectrum of spin waves. The spectral energy decomposition of a semi-bounded ferrimagnet is the sum of independent contributions from strongly nonlinear normal modes — solitons and magnons from the two branches of the dispersive wave spectrum. Discrete frequencies of the internal precession of solitons lie outside the region of the continuous spin wave spectrum. It is found that soliton nuclei are not rigid formations. When interacting with the sample surface, they undergo significant changes, which are accompanied by remagnetization of the surface layers of the material. Therefore, the particle-like excitations

we obtained cannot be described by previously known perturbative methods for solitons of an unbounded medium. Such assume small changes in the structure and properties of solitons under the action of perturbations. After the reflection from the surface, the resulting particle-like excitations, as they move deeper into the sample, acquire a stationary form, typical for the precessing solitons of an unbounded ferrimagnetic [9–11].

The position changes and initial phase shift of the internal oscillations of the soliton after its reflection from the edge of the sample are calculated.

The experimental confirmation of elastic reflection of solitons from the sample edge and observation of the processes of remagnetization of the boundary layers of the medium during the collision of a soliton with surface are relevant.

The results obtained should be taken into account when choosing a strategy for modeling soliton modes in real samples of finite sizes. They are useful for verification of numerical calculations. These results may serve as a basis for planning new experiments to study the nonlinear dynamics of bounded ferrimagnets under strong external forcing.

Acknowledgments

The author would like to express his gratitude to A.A. Raskovalov for constructive comments and assistance in preparing the manuscript for publication.

Funding

The study was made within the framework of the state assignment of the Ministry of Education and Science, topic „Quantum“ (number 122021000038-7).

Conflict of interest

The author declares that he has no conflict of interest.

References

[1] A.G. Gurevich. Magnetic resonance in ferrits and antiferromagnets. Nauka, M. (1973). p. 588. (in Russian).
[2] A.G. Gurevich, G.A. Melkov. Magnetization oscillations and waves. CRC Press, Boca Ration, FL, London (1996). 464 p.
[3] E.A. Turov, A.V. Kolchanov, V.V. Menshenin, I.F. Mirsaev, V.V. Nikolaev. Symmetry and the physical properties of antiferromagnets. Fizmatlit, M. (2001). p. 560. (in Russian).
[4] E.V. Gomonay, V.M. Loktev. Low Temperature Physics **40**, *1*, 17 (2014).
[5] B.A. Ivanov. Low Temperature Physics **45**, *9*, 935 (2019).
[6] V.G. Bar'yachtar, M.V. Chetkin, B.A. Ivanov, S.N. Gadetskii. Springer Tracts in Modern Physics **129**. Springer, New York (1994). 189 p.
[7] S.S. Dhillon, M.S. Vitiello, E.H. Linfield, A.G. Davies, M.C. Hoffmann, J. Booske, C. Paoloni, M. Gensch, P. Weightman, G.P. Williams, E. Castro-Camus, D.R.S. Cumming, F. Simoens, I. Escorcia-Carranzo, J. Grant, S. Lucyszyn, M. Kuwata-Gonokami, K. Konishi, M. Koch, C.A. Schmuttenmaer, T.L. Cocker, R. Huber, A.G. Markelz, Z.D. Taylor, V.P. Wallace, J.A. Zeitler, J. Sibik, T.M. Korter, B. Ellison, S. Rea, P. Goldsmith, K.B. Cooper, R. Appleby, D. Pardo, P.G. Huggard, V. Krozer, H. Shams, M. Fice, C. Renaud, A. Seeds, A. Stöhr, M. Naftaly, N. Ridler, R. Clarke, J.E. Cunningham, M.B. Johnston. J. Phys. D.: Appl. Phys., **50**, p. 043001 (2017).
[8] V.G. Bar'yakhtar, B.I. Ivanov. In the world of magnetic domains. Naukova dumka, Kiev (1986). p. 159. (in Russian).
[9] A.B. Borisov, V.V. Kiseliev, G.G. Talutz. Sol. St. Comm. **44**, *3*, 441 (1982).
[10] B.A. Ivanov, A.L. Sukstanskii. JETP **57**, *1*, 214 (1983).
[11] A.B. Borisov, V.V. Kiselev. Quasi-one-dimensional magnetic solitons. Fizmatlit, M. (2014). p. 520. (in Russian).
[12] V.V. Kiselev. JETP **163**, *3*, 330 (2023).
[13] V.V. Kiselev. Theoret. and Math. Phys. **219**, *1*, 576 (2024).
[14] V.V. Kiselev, A.A. Raskovalov. Chaos, Solitons and Fractals **188**, p. 115500 (2024).
[15] V.V. Kiselev. Theoret. and Math. Phys. **220**, *3*, 1440 (2024).
[16] E.A. Turov. Physical properties of magnetically ordered crystals. Academic Press, New York, London (1965). 222 s.
[17] Collected papers of L.D. Landau. Edited by D. Ter Haar. Pergamon press, s. 101 (1965).
[18] L.D. Landau, E.M. Lifshitz, L.P. Pitaevskii. Statistical Physics, part 2, Theory of the Condensed State, Volume 9 of Course of Theoretical Physics. Pergamon press (1980). 387 p.
[19] W.F. Brown. Micromagnetics. Springer Science and Business Media, New York: Interscience (1963). 143 p.
[20] S.V. Vonsovskii. Magnetism. J. Wiley, New York (1974). 1256 p.
[21] A.I. Akhiezer, V.G. Bar'yackhtar, S.V. Peletminskii. Spin waves. North–Holland Pub. Co., Amsterdam (1968). 372 p.
[22] I.V. Bar'yachtar, B.A. Ivanov. Sov. J. Low Temp. Phys. **5**, 361 (1979).
[23] F.D. Gakhov. Boundary value problems. Dover Publications Inc., New York (1990). 561 p.
[24] S.P. Novikov, S.V. Manakov, L.P. Pitaevskii, V.E. Zakharov. Theory of solitons. The inverse scattering method. Plenum, New York (1984).

Translated by A.Akhtyamov